



The effect of long-term service at elevated temperatures on structure and mechanical properties of Cr-Mo-V steel

J. Ówiek ^{a,*}, J. Łabanowski ^b, S. Topolska ^a

^a Institute of Engineering Materials and Biomaterials, Silesian University of Technology,
ul. Konarskiego 18a, 44-100 Gliwice, Poland

^b Faculty of Mechanical Engineering, Gdańsk University of Technology,
ul. Narutowicza 11/12, 80-233 Gdańsk, Poland

* Corresponding author: E-mail address: janusz.cwiek@polsl.pl

Received 06.02.2011; published in revised form 01.05.2011

ABSTRACT

Purpose: of this paper is to reveal the microstructural changes in 13HMF steel exposed to long-term service at elevated temperatures. The degradation of bainite structure was determined and carbides morphology has been examined. The influence of carbides evolution was discussed in dependence of creep rupture strength and mechanical properties of the steel.

Design/methodology/approach: Examinations were conducted on 273 mm diameter, 32 mm wall thickness tube made of 13HMF (14MoV6-3) steel. The tube was a segment of stem pipeline used in power plant at 540°C. The service time is 168,000 hours. Microstructure of the material has been examined with the use of light optical microscopy and scanning electron microscopy (SEM). The energy dispersive X-ray spectrometry (EDS) analysis was used for phase chemical composition identification. Transmission electron microscopy (TEM) of thin foils was used for carbides structure identification. The mechanical properties of the tube material were evaluated in static tensile tests at room temperature, hardness tests and impact Charpy U tests.

Findings: Microstructure of 13HMF steel tube shows an advanced level of degradation - coagulation of carbides at ferrite grain boundaries and inside bainitic grains. Precipitates of carbides decorated grain boundaries in chain forms. The presence of M_7C_3 , $M_{23}C_6$, M_6C phases were revealed. After extended service $M_{23}C_6$ and M_3C carbides were replaced by more stable carbides. This transformation did not occur until the end. This indicates the presence of mainly Mo_2C carbide, and only sporadic occurrence of carbide M_6C .

Practical implications: Useability of the method for assessing the current degradation level and for predicting residual lifetime of creep-resistant tubes based on analysis of carbides morphology was confirmed for Cr-Mo-V steel.

Originality/value: Information available in literature does not clearly indicate the influence of microstructure and mechanical properties of Cr-Mo-V steel after long-term exploitation. The study shows such relations.

Keywords: Creep-resistance; Structure degradation; Cr-Mo-V steel; Steam pipeline

Reference to this paper should be given in the following way:

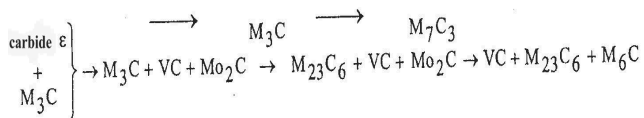
J. Ówiek, J. Łabanowski, S. Topolska, The effect of long-term service at elevated temperatures on structure and mechanical properties of Cr-Mo-V steel, Archives of Materials Science and Engineering 49/1 (2011) 33-39.

PROPERTIES

1. Introduction

Low-alloy Cr-Mo-V steels are widely used in power generation industry, mainly for steam pipelines, boiler and turbine parts working at elevated temperature and under high pressure. Such working conditions causes changes in their microstructure and in consequence deterioration of their functional properties. Decrease of creep resistance of the steel is a result of structural changes in matrix and due to precipitation reactions. The main parameters influencing steels creep resistance are: chemical composition modifications and accompanied heterogeneity in solid solution, changes in dislocation structure and dislocation density and growth, secondary carbides precipitation and interactions with primary carbides, carbides transformations and precipitation of intermetallic phases, Changes in phase morphologies. Creep tests results and observations of Cr-Mo-V steels after long-term exploitation at elevated temperatures indicate that carbide morphology and their transformations have the fundamental influence on steel properties.

In bainite matrix microstructure of Cr-Mo-V steels carbide transformations are complex and proceed with appearance of intermediate phases. Throughout whole exposure time stable VC carbides dominates in the structure. Other carbides like M_3C and Mo_2C undergo changes into M_6C after a sufficiently long time. The chemical composition of the matrix also changes. Transformations of carbides morphology in Cr-Mo-V steels occur in sequence:



The objective of this study is to show the influence of the service exposure on mechanical properties and carbide morphology in 13HMF steel.

2. Experimental

Examinations were conducted on one segment of $\varnothing 237 \times 32.0$ mm fresh steam pipeline connecting the steam boiler with turbine. Tube was made of 13HMF according to PN-75/H-84024 (14MoV6-3 according to PN-EN10216-2) steel grade and was operated for approximately 168 000 hours at 540°C under 14 MPa pressure. The chemical composition of tested steel is given in Table 1.

Table 1.
Chemical composition of tested 13HMF steel (14MoV6-3)

wt. %							
C	Si	Mn	P	S	Cr	Mo	V
13HMF acc. to PN-75/H-84024							
0.10-0.18	0.15	0.40	max	max	0.30	0.50-0.65	0.22
	0.35	-0.70	0.040	0.040	0.60	0.65	0.35
tested tube $\varnothing 237 \times 32.0$ mm							
0.15	0.28	0.36	0.005	0.020	0.33	0.51	0.26

2.1. Microstructure

Tube wall thickness was uniform on the perimeter and averaged 31.8 mm. On the inner tube surface the uniform corrosion was observed in a form of compact layer, strictly adhering to the metal surface. There were no defects such as cracks or voids and the occurrence of pitting corrosion. The NDT magnetic tests confirmed good condition of tested tube. Inner and outer surfaces of tube were checked with the use of magnetic particle and ultrasonic testing. Not the type of discontinuity has been detected like outside and subsurface cracks (to a depth of about 2.5 mm).

Metallographic studies were performed on specimens taken into transverse and longitudinal direction of tube axis to check the microstructure and its degradation level occurred during long term exploitation.

The severity of non-metallic inclusions was defined according to PN-64/H-04510 standard. Contamination of non-metallic inclusions was on an acceptable level. The non-metallic particles occur in the form of separate oxides, no sulphides were detected.

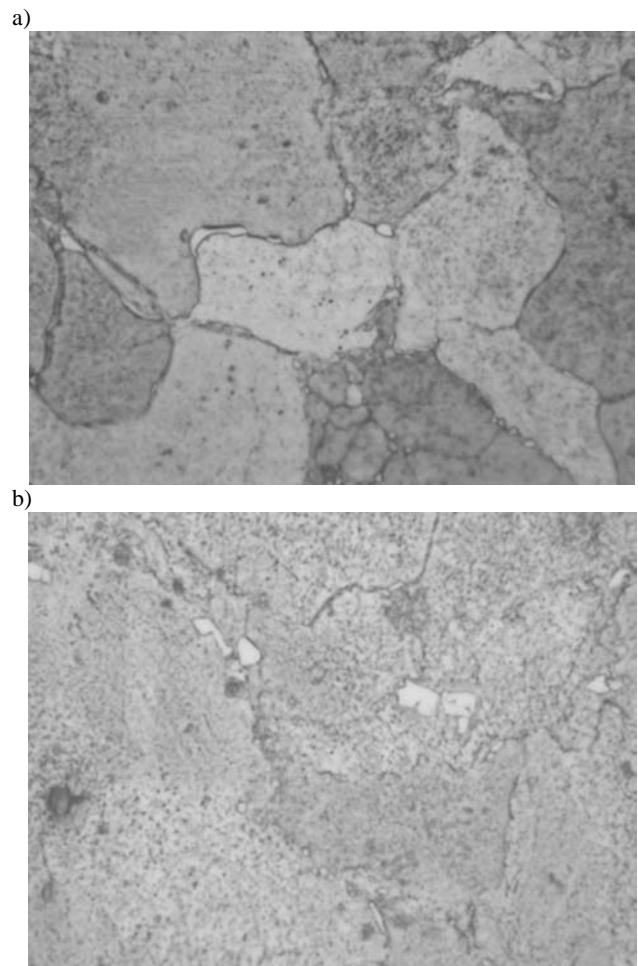


Fig. 1. Microstructure of 13HMF steel tube $\varnothing 273 \times 32$ mm, Magn. 1000x

The degradation level of tube microstructure was determined by comparison with the scale models [10]. The extent of degradation of the carbide structure for steel 13HMF (14MoV6-3) was performed at magnification of 500 and 1000x. Observations were conducted on an light microscope Leica MEF4M.

The structure of the tube material has an advanced degree of degradation. On Fig. 1 it can be seen separate coagulated cementite particles and carbides at the grain boundaries of ferrite and bainite areas. Visible are large single precipitates and precipitates occurring in the form of strings deployed along the grain borders. Assessment of structure degradation according to the criteria [10] corresponds to the model of SIII. There were no decohesion changes in the tube steel microstructure.

2.2. Mechanical properties

Vickers hardness test has been performed according to standard PN-EN ISO 6507-1 along the tubes wall cross section. Results of hardness test are shown in Table 2. The average hardness of the tube material of 146 HV, corresponds to the degree of degradation according to the criteria SIII [10].

Table 2. Results of Vickers hardness test on the cross section of tube wall

	Hardness HV10						
	outer surface ----->			inner surface			
No	1	2	3	4	5	6	7
HV10	150	148	148	148	148	148	148
No	8	9	10	11	12	13	14
HV10	145	143	143	143	143	143	143
No	15	16	17	18	19	20	21
HV10	145	145					

Tensile tests were performed on the round samples with gauge diameter of 10 mm machined from tubes wall. Yield strength (YS), tensile strength (TS), and elongation (EL) were recorded and compared to the PN-85/H-74252 standard requirements for new material. Results of tests are shown in Table 3. Tube material after period of exploitation shows good mechanical properties. Tensile stress fulfills the standards requirements on the basic level but proof stress seems to be unsatisfactory.

Table 3. Results of static tensile tests

Sample	YS MPa	TS MPa	EL %
13HMF PN-85/H-74252	min 365	490-690	min 20
Sample 1	287	490	29.0
Sample 2	297	494	28.6
Average	292	492	28.8

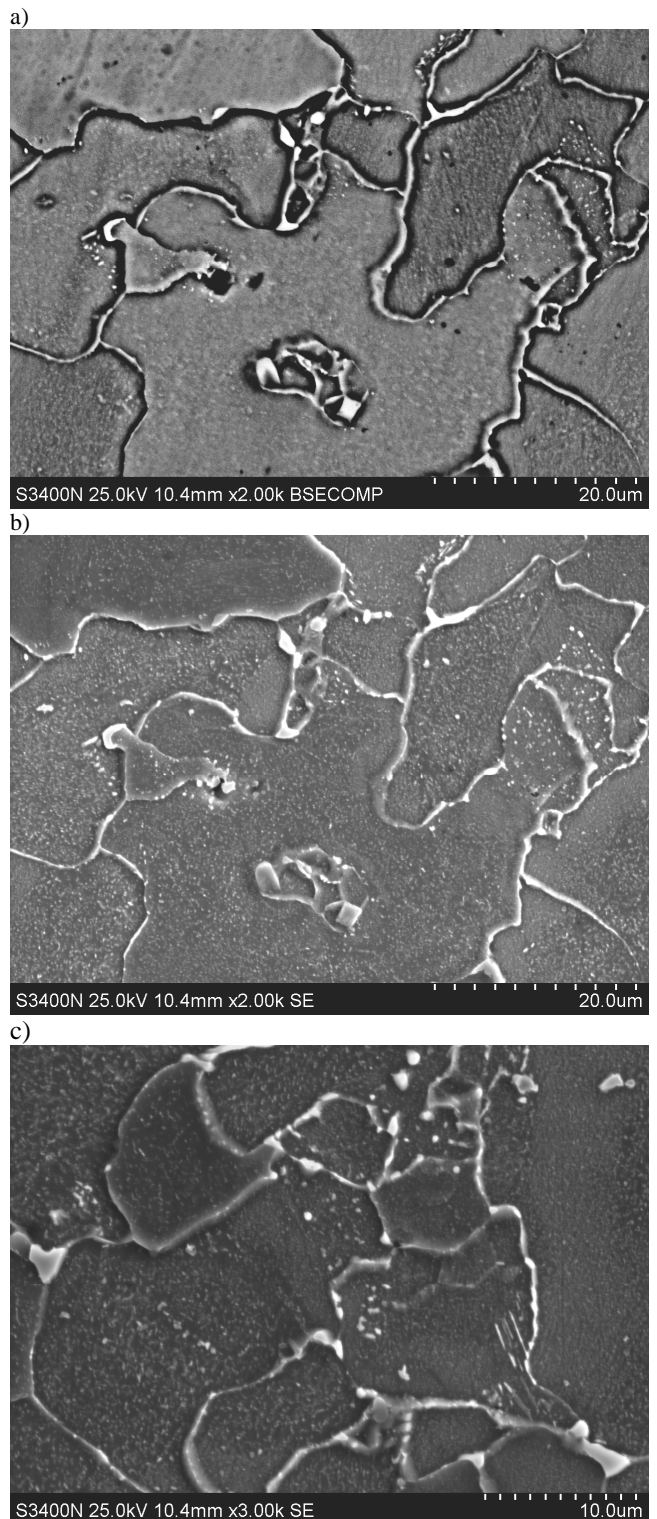


Fig. 2. Carbides morphology in 13HMF steel, tube Ø 273 × 32 mm. Observations performed at metallographical samples SEM, detector: a) BSE, b), c) SE

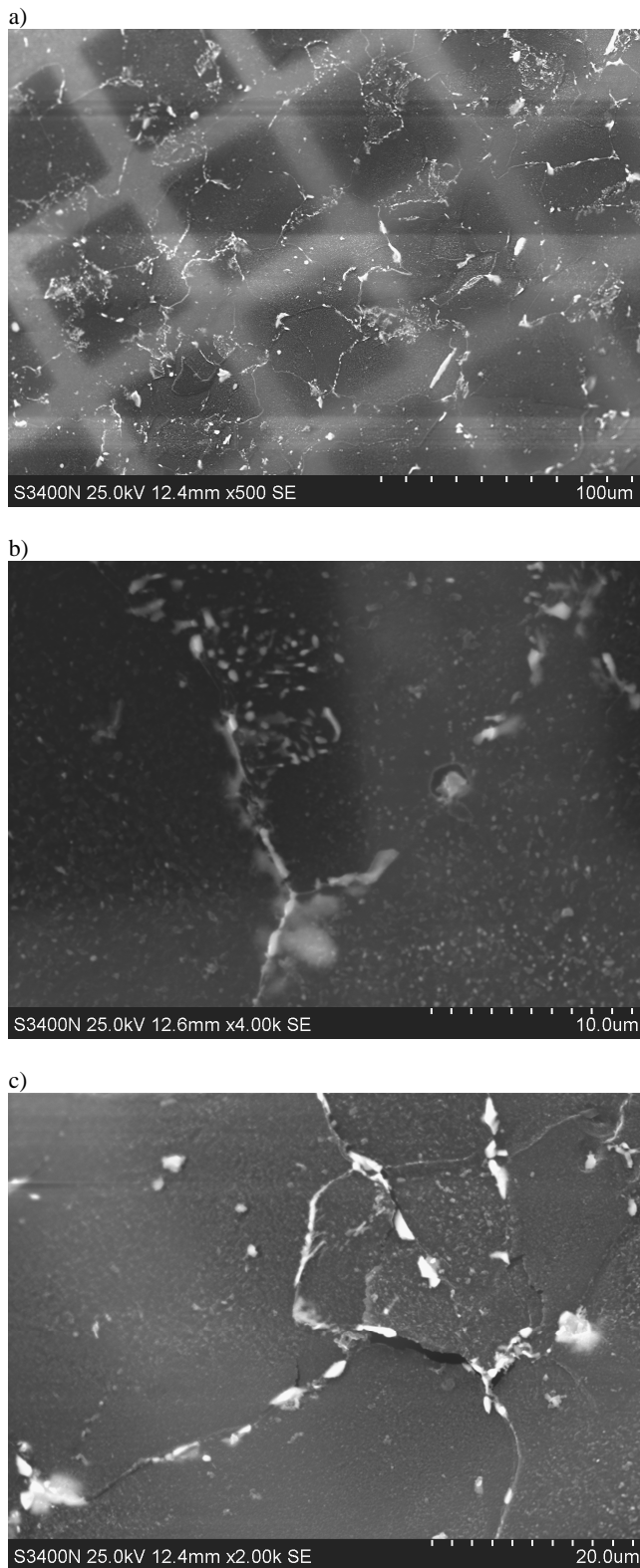


Fig. 3. Carbides morphology in 13HMF steel, tube $\varnothing 273 \times 32$ mm. Extraction replica, SEM, detector SE

Charpy U impact tests were performed at room temperature ($+20^{\circ}\text{C}$). The specimens were taken in the longitudinal and transverse direction of the tube axis. Impact tests were performed according to PN-EN 10045-1 standard. Test results with comparison to PN-85/H-74252 standard requirements are shown in Table 4.

Tube material meets the requirements of a excess to standards requirements on both the sample longitudinal and transverse.

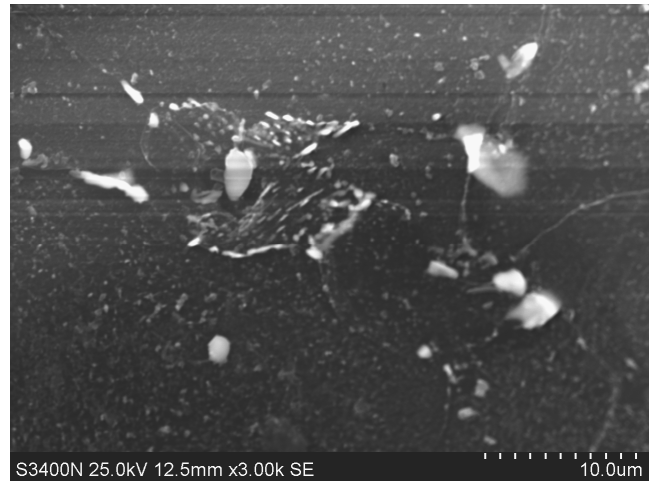


Fig. 4. Carbides morphology in 13HMF steel microstructure, tube $\varnothing 273 \times 32$ mm. Extraction replica, SEM, detector SE

Table 4.

Results of Charpy U impact tests. Average results from 3 samples

Sample	KCU2	KCU2
	J/cm ² longitudinal	J/cm ² transverse
13HMF PN-85/H-74252	min. 88	min. 59
Tube $\varnothing 273 \times 32$ mm	181	139

2.3. Carbides morphology investigations

Investigations were performed for:

- determine the morphology and chemical composition of carbides in the scanning electron microscope (SEM) with EDS attachment,
- determine the crystal structure and identification of carbides with the use of transmission electron microscope (TEM).

SEM examinations of carbides morphology and chemical composition

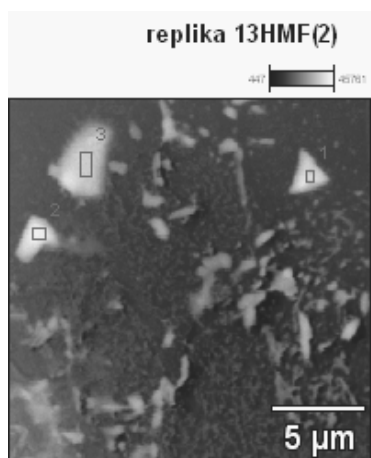
Carbide morphology was performed on scanning electron microscope (SEM) Hitachi S3400N using SE and BSE detectors. SE detector creates an image in secondary electron reflecting surface topography. BSE detector forming the image in

backscattered electrons and further highlights the contrast depends on differences in chemical composition of the different areas of the image. Quantitative chemical analysis in microareas (carbides) was performed on the scanning electron microscope with an attachment to the X-ray microanalysis EDS.

The study was conducted on two types of samples:

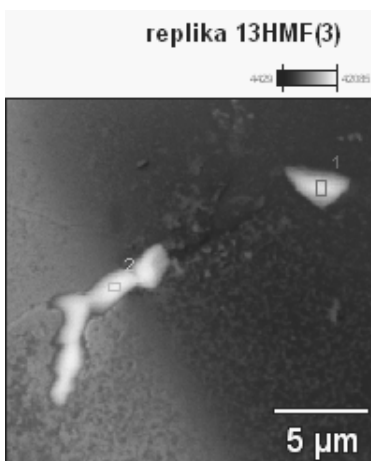
- metallographic samples,
- extraction replicas removed from the surface of metallographic cross-sections.

Morphology of carbides observed on metallographic samples is shown in Fig. 2. Many small carbides are visible - dispersed inside the degraded bainite grains and relatively large carbides at grain boundaries, which often form a continuous net.



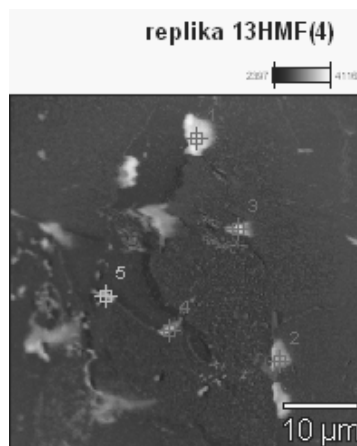
Weight %

Point	V-K	Cr-K	Mn-K	Fe-K	Mo-L
pt1	0.67	7.61	6.94	70.18	14.60
pt2	1.09	7.75	7.34	70.39	13.43
pt3	1.50	7.81	8.00	73.00	9.68



Weight %

Point	V-K	Cr-K	Mn-K	Fe-K	Mo-L
pt1	1.14	7.09	8.25	68.51	15.02
pt2	0.80	7.24	7.58	71.15	13.24



Weight %

Point	V-K	Cr-K	Mn-K	Fe-K	Mo-L
pt1	1.65	7.07	7.29	69.83	14.15
pt2	2.20	7.43	7.53	69.38	13.45
pt3	1.47	7.12	7.64	69.07	14.69
pt4	1.28	6.81	8.43	67.67	15.81
pt5	1.56	7.50	7.56	65.60	17.78

Fig. 5. EDS chemical microanalysis and morphology of carbides in 13HMF steel, tube $\varnothing 273 \times 32$ mm. Extraction replica, SEM, detector SE

Carbides morphology disclosed on a replica is shown in Figs. 3,4.

Example results of chemical composition investigations of carbides are presented in Fig. 5. It was found that carbide content by weight is about: 14% Mo, 8% Mn, 7% Cr and 1% V. It should be noted that the EDS analysis of low volume carbide precipitates is a qualitative analysis and does not give the exact chemical composition of the phase only by informing the elements are present.

TEM examinations of carbides morphology and chemical composition

Structural studies, including analysis of phase composition was performed using a JEOL 100B transmission electron microscopy operating at 100 kV accelerating voltage. Research was conducted on extraction replicas and thin foils. Diffraction studies were performed using selective diffraction. Constant microscope (λL) was determined from the standard sample. In order to analyze the phase composition, the lattice crystallographic system was generated by entering the number of atoms in the unit cell and their x, y, z positions. After loading the data described above, unit cell parameters was described (lattice parameters a, b, c, angles between them of α , β , γ , and a minimum interplanar distance d). After indexing diffraction lines the B direction was determined.

Figures 5-9 show the shape of precipitates and diffraction patterns of determined carbides.

TEM examinations revealed the presence of the following phases in 13HMF steel microstructure: MX , M_2X , M_7C_3 , $M_{23}C_6$, M_6C , where X is a non-metal such as C or N. The presence of M_6C carbide is disclosed a single case. There is a simultaneous occurrence of

partial areas of the MX M_2X in the matrix, but there are other areas with only the MX precipitates. M_7C_3 precipitates occur at grain boundaries and inside grains as well as precipitates of $M_{23}C_6$ carbides. $M_{23}C_6$ phase observed in the areas of grain boundaries are often defected and have irregular shapes. They are rarely seen inside the grains. Local areas free of dislocations and precipitates, and showing the effects of high-angle grain boundary migration were no detected. In many areas, the process of forming cellular structures were found (built with dislocation tangles). Dislocations uniformly distributed in the matrix are blocked by the fine particles of MX and M_2X phases.

3. Discussion

Mechanical properties of tube material after service period of 168,000 hours at 540°C are only at the acceptable level. In comparison to the as received material, both tensile strength and hardness decreased considerably when elongation and impact strength remain as satisfactory.

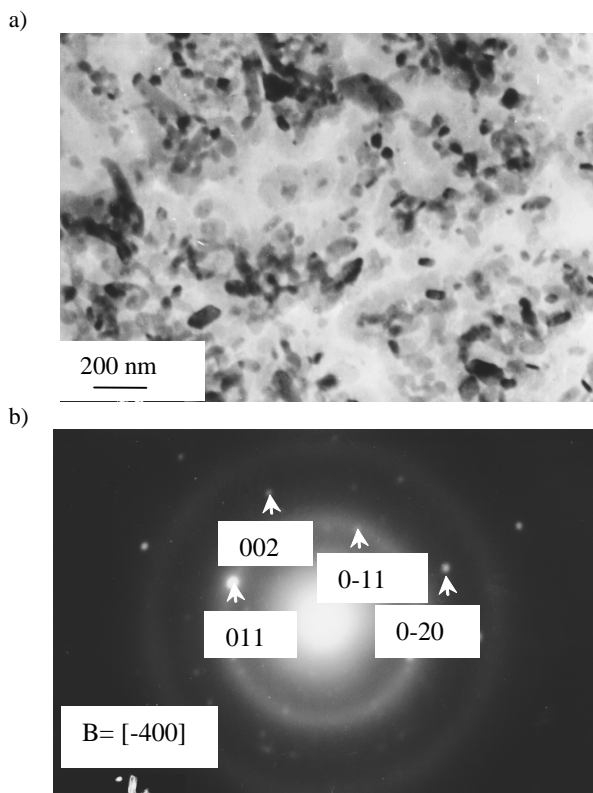


Fig. 5. a) Dispersed MC precipitates, TEM image b) Diffraction pattern of MC precipitates

13HMF (14MoV6-3) steel tube microstructure shows an advanced level of degradation. Carbides coagulation process occurs at ferrite grain boundaries and in bainite areas. Precipitates are in the form of chains and large, separate particles along the grain boundaries. Evaluation of degradation of the tubes structure according to the criteria [3] based on light microscopy

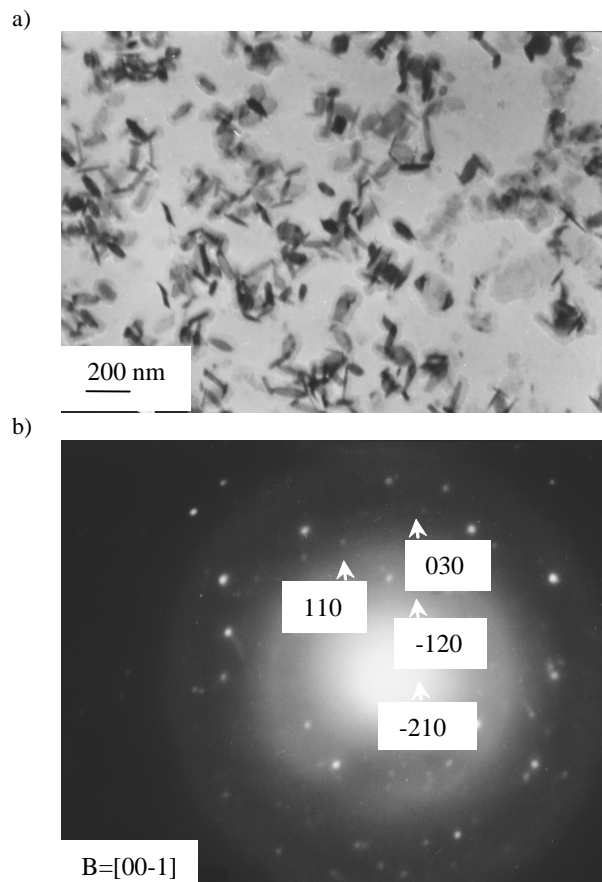


Fig. 6. a) Dispersed M_2C precipitates, TEM image b) Diffraction pattern of M_2C precipitates

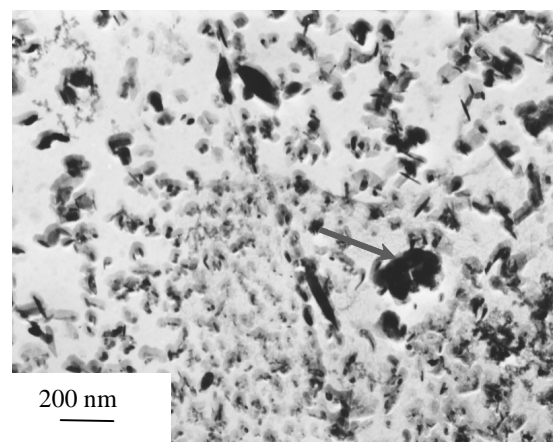


Fig. 7. The diverse morphology of the precipitates. Arrow marked the precipitation where the diffraction was performed

observations corresponds to the model SIII. Morphology, structure and chemical composition of carbides determined in SEM and TEM investigations confirmed the advanced

degradation of the microstructure. The presence of M_7C_3 , $M_{23}C_6$, M_6C phases were revealed. After extended service $M_{23}C_6$ and M_3C carbides were replaced by more stable carbides. This transformation did not reach the end, i.e. degradation process is not in final stage which is characterized by occurrence of creep micro-voids. This indicates the presence of mainly Mo_2C carbide, and only a few of M_6C carbides.

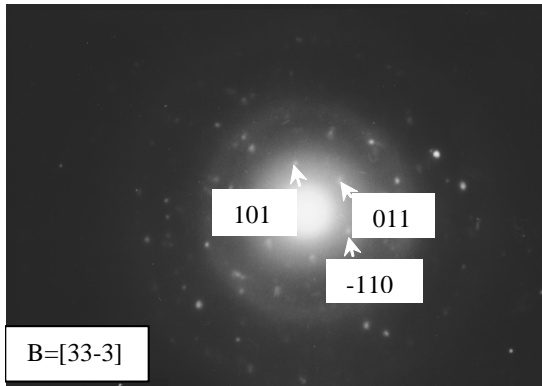


Fig. 8. Diffraction pattern of particle shown by arrow in Fig. 7, $M_{23}C_6$ precipitate

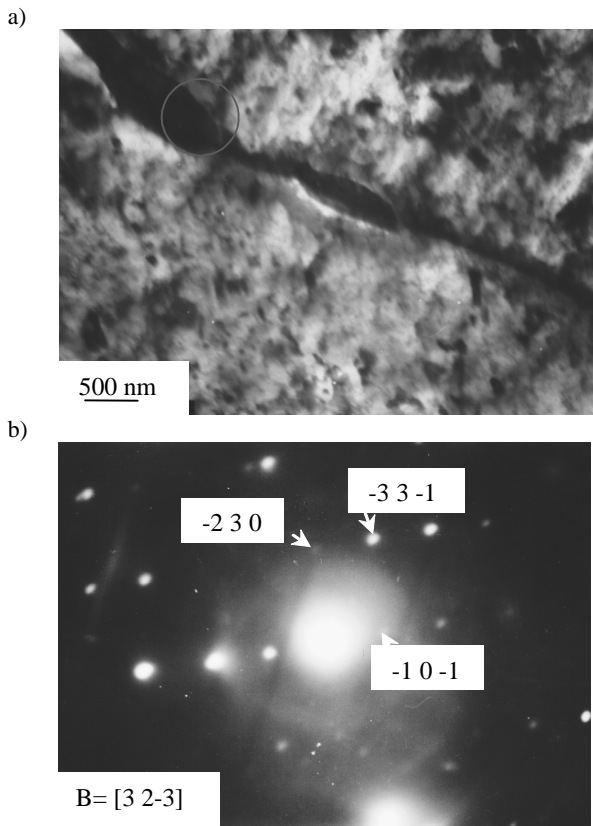


Fig. 9. a) Dispersed M_7C_3 precipitates, TEM image b) Diffraction pattern of M_7C_3 precipitates

4. Conclusions

Determination of a Cr-Mo-V steel microstructure degradation, after long-term service at elevated temperature, requires conduction of wide range investigations including mechanical, metallographic, structural, and chemical analysis tests [13-15].

The tested 13HMF (14MoV6-3) steel steam pipeline shows an advanced level of degradation after service period of 168,000 hours at 540°C.

Carbides coagulation process occurs at ferrite grain boundaries and in bainite areas. The presence of M_7C_3 , $M_{23}C_6$, M_6C phases were revealed.

But degradation process is not in final stage yet, which has been proofed by presence of mainly Mo_2C carbides, and only a few of M_6C carbides. There were no creep micro-voids in the tube.

References

- [1] A. Hernas, Creep resistance of steel and alloys, Silesian University of Technology, Gliwice, 1999 (in Polish).
- [2] G. Y. Lai, High-temperature corrosion of engineering alloys, ASM International (1997).
- [3] Metals Handbook, Failure Analysis and Prevention. ASM International 11 (1995).
- [4] Metals Handbook, Corrosion, ASM International 13 (1987).
- [5] Atlases - changes in microstructure of creep resistant steels due to long term use. Institute of Power Energy, Warsaw, 1996.
- [6] J. Nowacki, P. Rybicki, Corrosion resistance of SAW duplex joints welded with high heat input, Journal of Achievements in Materials and Manufacturing Engineering 23/2 (2007) 7-14.
- [7] J. Łabanowski, S. Topolska, J. Ćwiek, Assessment of evaporator tubes corrosion in low-emission steam boilers Advances in Materials Science (online), Versita, Warsaw 8/4 (2008) 14-21.
- [8] J. Okrajni, K. Mutwil, M. Cieśła, Steam pipelines effort and durability, Journal of Achievements in Materials and Manufacturing Engineering 22/2 (2007) 63-66.
- [9] S. Mrowec, T. Weber, The modern heat resistant materials, WNT, Warsaw, 1982 (in Polish).
- [10] A. Zieliński, J. Dobrzański, G. Golański, Estimation of the residual life of L17HMF cast steel elements after long-term service, Journal of Achievements in Materials and Manufacturing Engineering 34/2 (2009) 137-144.
- [11] D. Renowicz, A. Hernas, M. Cieśła, K. Mutwil, Degradation of the cast steel parts working in power plant pipelines, Journal of Achievements in Materials and Manufacturing Engineering 18 (2006) 219-222.
- [12] J. Okrajni, Thermo-mechanical fatigue conditions of power plant components, Journal of Achievements in Materials and Manufacturing Engineering 33/1 (2009) 53-61.
- [13] J. Ćwiek, Plasma nitriding as a prevention method against hydrogen degradation of steels, Journal of Achievements in Materials and Manufacturing Engineering 36/1 (2009) 25-32.
- [14] J. Ćwiek, M. Baczyńska, Behaviour of nitrided layers subjected to influence of hydrogen, Archives of Materials Science and Engineering 43/1 (2010) 30-41.
- [15] J. Ćwiek, Plasma Prevention methods against hydrogen degradation of steel, Journal of Achievements in Materials and Manufacturing Engineering 43/1 (2010) 214-221.